General Disclaimer

One or more of the Following Statements may affect this Document

- This document has been reproduced from the best copy furnished by the organizational source. It is being released in the interest of making available as much information as possible.

- This document may contain data, which exceeds the sheet parameters. It was furnished in this condition by the organizational source and is the best copy available.

- This document may contain tone-on-tone or color graphs, charts and/or pictures, which have been reproduced in black and white.

- This document is paginated as submitted by the original source.

- Portions of this document are not fully legible due to the historical nature of some of the material. However, it is the best reproduction available from the original submission.

NASA Technical Memorandum 83386

Pore Size Engineering Applied to the Design of Separators for Nickel-Hydrogen Cells and Batteries

Kathleen M. Abbey and Doris L. Britton
Lewis Research Center
Cleveland, Ohio

Prepared for the
Eighteenth Intersociety Energy Conversion Engineering Conference
cosponsored by the AIChE, IEEE, AIAA, ACS, ANS, ASME, and SAE
Orlando, Florida, August 21–26, 1983

NASA

PORE SIZE ENGINEERING APPLIED TO THE DESIGN OF SEPARATORS FOR NICKEL-HYDROGEN CELLS AND BATTERIES

Kathleen M. Abbey and Doris L. Britton

National Aeronautics and Space Administration
Lewis Research Center
Cleveland, Ohio 44135

E-1663

ABSTRACT

Pore-size engineering in starved alkaline multiplate cells involves adopting techniques to widen the volume tolerance of individual cells. This is accomplished by designing separators with appropriate pore-size distributions and wettability characteristics (capillary pressure considerations) to have wider volume tolerances and an ability to resist dimensional changes in the electrodes. The separators studied for potential use in nickel-hydrogen cells reported here consist of polymeric membranes as well as inorganic microporous mats. In addition to standard measurements, the resistance and distribution of electrolyte as a function of total cell electrolyte content have been determined.

New composite separators consisting of fibers, particles and/or binders deposited on Zircar cloth have been developed in order to engineer the proper capillary pressure characteristics in the separator. These asymmetric separators have been prepared from a variety of fibers, particles and binders.

INTRODUCTION

Maximizing performance in starved multi-plate cells involves adopting techniques to widen the volume tolerance of individual cells and components within the cells. These techniques rely on introducing electrolyte reservoirs into the cells and taking advantage of the capillary characteristics of all the components and their interactions. These methods have been applied to a variety of fuel cell systems including alkaline fuel cells. While some similarities exist between starved electrolyte batteries and fuel cells, multiplate nickel-hydrogen cells differ from fuel cells in the following ways: (1) reactions and transport of water proceed in only one direction in fuel cells, whereas in batteries, the reactions and transport reverse. (2) In nickel-hydrogen cells, the pore characteristics and dimensions of the electrode change with cycling. (3) A larger percentage of the electrolyte in fuel cells resides in separators and reservoirs rather than in electrodes. In nickel-hydrogen cells, the electrolyte is almost entirely distributed between the nickel electrode and the separator with a relatively small amount found in the hydrogen electrode. General approaches to widening separator volume tolerance have been discussed previously [1] as well as requirements of different battery systems [2] and so will only be summarized here.

The resistance of any component in a cell varies with the electrolyte content of the component. For porous components not involved in gas reactions, generally the greater the amount of electrolyte, the lower the resistance. For gas electrodes, a critical balance among the gas, electrolyte and catalyzed surface must be maintained for the electrode resistance to be minimized. When components are assembled to form cells in multiplate cells and batteries which do not operate with an excess of electrolyte, the electrolyte redistributes among the components so that at equilibrium, the capillary pressures are equal. For nickel-hydrogen cells and batteries this becomes

$$P_{H2} = P_{sep} + P_{Ni} = P_{reservoir\ plate} \quad (1)$$

Reservoir plates are not always included in all designs. The capillary pressure is given by

$$p = \frac{2\gamma \cos\theta}{r} \quad (2)$$

where γ is the electrolyte surface tension in the pores, r is the pore radius and θ is the contact angle which the electrolyte makes with the pore walls, it can be seen that at equilibrium, pores of the same size and wettability will be filled in all porous components which are in contact and consequently, the pore size distribution, percent porosity and wettability all contribute to the percent filling of the porous component. The goal is to optimize the electrolyte content in each cell component for minimum resistance, and in each cell for maximum performance.

Because the parameters of each porous component may vary the optimum electrolyte volume for each component will assume a distribution of values. Thus cells in a stack of cells will be characterized by a distribution of optimum electrolyte volumes. Because the cell filling procedures typically utilized cannot insure that each plate in a multiplate cell is filled with an optimum volume of electrolyte, most cells will be

filled either on the wet or dry side of the optimum volume value. Figure 1 shows a possible distribution of cell values for nickel-hydrogen cells based on a distribution of electrolyte in each cell.

The design of new components for nickel-hydrogen cells must focus on developing components with resistances less sensitive to cell electrolyte content. Generally, microporous separators are preferred for starved electrolyte cells where dendrite growth is absent. The reasoning may be explained as follows: Charging and discharging cycles differ not only in length of time, but in competing side reactions as well [2]. Some phenomena such as water accumulation in different locations of the cell become cumulative after many cycles [3]. Electro-osmotic effects are often important in flooded cells using ion-exchange membranes as battery separators [3-4]. Here, the high charge densities in the pores of the separator accentuate any imbalances which occur between charging and discharging.

Microporous separators generally exhibit smaller charge densities on the pore walls and thus, the electrode dimensional changes must also be considered when designing new separators for cells. Nickel electrodes in cycled cells typically exhibit up to a ten percent change (increase) in porosity [5], a large change in pore surface area [6] and an increase in small pores and in pore size distributions. Changes in the nickel electrode structure either compress the separator and/or remove electrolyte through changes in capillary pressure. As the electrode thickness increases, the separator must be able to accommodate the additional compression and resultant loss of electrolyte. Equally important to the physical structure are problems of fabrication and transport phenomena which occur when all components are grouped together in the cell.

The basic approach to separator design may be summarized as follows:

(a) Pore size distributions are determined in electrodes and separators.

(b) Prediction of electrolyte distribution among cell components is based on these measurements using principles of equalization of the capillary pressure values.

(c) Actual electrolyte distribution among the cell components is measured.

(d) Resistance is measured as a function of component compression.

(e) Resistance is measured as a function of electrolyte content.

(f) Observations are correlated with wettability and pore size.

(g) New separators are designed based on those results.

EXPERIMENTAL

Approaches to Microporous Separator Fabrication

Most materials used to form microporous separators have traditionally been metal oxide fibers and particles, such as TiO_2, CeO_2, $Mg(OH)_2$, ZrO_2, Al_2O_3 and asbestos. All of these compounds contain surface oxygen groups which can hydrogen bond to water or with electrolyte solution. Consequently, the surface groups are then hydroxyl groups and the surfaces are strongly basic. Charges are actually developed on the surfaces by further reaction with hydroxyl groups [7], e.g.,

$$ZrO_2 + OH^- \longrightarrow ZrO \cdot OH \qquad (3)$$

$$ZrOOH \cdot OH^- \longrightarrow Zr(OH)_2 \cdot \qquad (4)$$

Because these reactions involve hydroxyl ions, the amount of surface charge developed is pH dependent. Associated with this charge is the potential difference developed between the plane of shear of the particle or fiber and the bulk solution. This potential difference is referred to as the zeta potential. For metal oxides, zeta potentials are of the order of millivolts. Because surface charges are pH dependent, the zeta potentials will be pH dependent as is shown in Figure 2 [7]. The larger the magnitude of the zeta potential, the stronger will be the repulsion between the particles. Hence, from the standpoint of fabrication, zeta potentials of particles must be minimized [8]. The isoelectric point is defined as the pH where the zeta potential is zero or where the number of positive surface charges equals the number of negative surface charges. Table I (7) lists the point of zero charge of several colloidal materials which might be used in the preparation of microporous separators. The history of preparation and exposure to a variety of cleaning conditions can affect the isoelectric point by several pH units [9]. When several fibers or fillers with different isoelectric points are combined together to form separators, the pH of the slurry solution will have to be adjusted to obtain optimum fabrication conditions.

These optimum solution conditions may be difficult to achieve in practice, or, the fibers may not adhere well due to a physical constraint such as brittleness. In many examples of state-of-the-art preparation of separators, binders which are resistant to alkaline electrolyte have been used to hold the fibers and particles together.

Binders

Interactions between unlike molecules such as a binder and a fiber are divided into primary binding forces such as reactions of polymers with metals through coupling agents, and secondary interactions such as dispersion forces, dipole-dipole forces, dipole-induced dipole forces, hydrogen bonding and acid-base interactions. Of these secondary interactions, the strongest are hydrogen bonding and acid-base

interactions. Binders which can act as acids would be expected to act as very strong adhesives to the basic metal oxide fibers used. We have, therefore, attempted to compare the effects of binders having strong hydrogen bonding forces with those having weak forces. These will be discussed in the section concerning microporous mats.

Measurements on Membrane Separators

Membrane separators have generally been made microporous by using synthetic polymeric fibers or by introducing holes into films by mechanical means. The commercial examples studied included wettable Celgard 3501, microporous polysulfone membranes (Gelman Sciences), Acropore NF-WA (Gelman Sciences), polyethylene (W. R. Grace Interseparator), and wettable polypropylene. Table II lists some of the characteristic membrane properties. The pore size distribution and electrolyte management characteristics of the latter two membranes have been discussed [2]. Additional measurements have been made so that these separators may be compared with the others studied.

The electrolyte distribution measurements among a series of cell components consisting of a nickel electrode, a hydrogen electrode, and a separator were made using a modified standard method [2,10,11]. The nickel and hydrogen electrode were obtained from boiler plate cells built by Eagle-Picher to Air Force specifications [12]. Electrodes were taken from a cell which had been disassembled after a few cycles and from another cell which had been cycled for approximately 2600 cycles. The components were assembled in a Plexiglass cell with the number of layers of separator adjusted so that the amount of electrolyte at one hundred per cent filling was similar from experiment to experiment. The cell was vacuum-filled to determine the one hundred percent fill condition, and then disassembled. The components were rinsed and dried in an oven. The cell was reassembled and progressively filled with electrolyte. Electrolyte content and resistance of each component were then measured incrementally at each step. Celgard, polypropylene, and polyethylene all show a loss of potassium hydroxide electrolyte to the nickel electrode. This is demonstrated in Table III where selected values have been shown. The electrolyte content of the nickel electrode remains relatively constant while the electrolyte content of the separator is far more sensitive to cell electrolyte content. Figures 3 and 4 show the electrolyte distribution curves for polysulfone and Acropore NF-WA. It can be seen that the polysulfone competes well with the nickel electrode for available electrolyte. Figures 5-9 show resistance as a function of electrolyte content for the membranes. Both Acropore NF-WA and polysulfone exhibit lower resistances which are relatively constant with electrolyte filling.

Inorganic Microporous Mats

The microporous mats studied were prepared by filtering a slurry of inorganic particles and fibers onto an evacuated sheet mold. Results from the standard separator tests are given in Table II. The mats studied included fuel cell grade asbestos with a butyl latex binder (relatively hydrophobic) and fuel cell grade asbestos with ethylene acrylic acid copolymer (hydrophobic and hydrophilic regions) used as a binder. Figures 10-12 show electrolyte distribution curves for these separators. Additional data is given in Table IV. From the curves it is evident that the butyl latex rubber (EBL) content progresses through a maximum value. The mat containing 10% EBL competes less well for electrolyte than the mat containing 5% EBL. This is confirmed by the flooded resistance measurements in Table II which show that the 10% EBL mat is more resistive. The mat which contains ethylene acrylic acid copolymer appears to compete more successfully for electrolyte over a range of electrolyte contents.

Attempts at Lewis Research Center to find an asbestos substitute have concentrated on blends of potassium titanate, zirconium oxide and binders. Preliminary measurements indicate that the pore size distribution achieved with these mixtures of materials are similar to those exhibited by asbestos with binders. Figure 13 and 14 show the pore size distributions of 80% potassium titanate, 20% zirconium oxide fibers and 10% EBL free-standing and layered onto Zircar Cloth. The pore size distribution of a Zircar cloth separator has also been given because Zircar has been identified as exhibiting good electrolyte retention characteristics [2]. It is evident that the pore size distribution of the composite separator is a mixture of the pore size distributions of the Zircar cloth and the free standing mat. The electrolyte distribution curve for this sample is shown in Figure 15 where it can be seen that the layered structure competes well for the available electrolyte.

Additional composite separators composed of fuel cell grade asbestos with binders deposited on Zircar cloth have been prepared. Electrolyte management curves are shown in Figures 16-18.

DISCUSSION

The polysulfone membranes appear to exhibit the best electrolyte management properties of the commercial membranes studied. In addition, a high bubble pressure and low flooded resistivity are properties of this separator. The resistance remains low as a function of electrolyte content which makes this material very attractive as a potential separator in nickel-hydrogen cells. However, it should be noted that properties of layered membranes are not strict multiples of single layers. For Celgard, e.g. the electrolyte content of twelve layers is much less than the electrolyte content of twelve single layers whereas the resistance is more than a factor of

twelve higher.

Use of ethylene-acrylic acid copolymer as a binder appears to enhance electrolyte management properties of fuel cell grade asbestos. The ethylene-acrylic acid is a random copolymer containing 15-20% by weight acrylic acid moieties. Present in a dispersion and under certain conditions of pH and concentration, the polymer will be fully extended. As the pH of a slurry of ethylene-acrylic acid and basic fibers such as the silicates which form asbestos changes the acrylic acid moieties should form strong bonds with the metal oxide fibers. Eventually, the ethylene-acrylic acid copolymer will precipitate out entirely with the fibers. The mat thus formed should have a strong integrity while being handled. When placed in a cell, the carboxylic acid groups should allow a high retention of electrolyte in the separator, further enhancing the pore structure of the microporous separator.

The conditions for formation of these separators must be carefully controlled because as the pH changes, the conformation of the ethylene-acrylic acid copolymer will vary from fully extended molecules to those conformations where the acrylic acid moieties are concentrated in regions or domains. The layered structures were fabricated in order to incorporate both large and small pore size distributions into the separators. High bubble pressures should be retained while enhancing the reservoir capabilities of the separators. Ethylene acrylic acid copolymer contents of 5-10% for the asbestos binders appear to lower the resistances of the composite separators when compared to butyl latex rubber. Further testing in cells is required before final conclusions can be drawn. However, systematic trends can be seen from the characterizations presented in this paper.

Separators differ in the amount of electrolyte retained when subjected to compressive forces. Table IV illustrates this by detailing the amounts of electrolyte measured in the separator after it had been placed in a cell with both nickel and hydrogen electrodes. These values may be compared with somewhat crude predictions based on the physical size (wet and dry) and measured porosity of the separators. It is clear that when the cells are assembled "finger-tight" that enough force is present to compress the separators to some degree. The resistance as a function of electrolyte content graphs shown in Figures 5-9 were all measured with the forces of compression resulting from assembly of the Plexiglass cells. More systematic studies of the effects of compression are currently under investigation.

CONCLUSIONS

a) Recommendations for cell testing of materials focuses on separators with improved electrolyte management characteristics.

b) Polysulfone membranes appear most promising of commercial membranes tested. Other commercial separators of synthetic materials which have been made wettable by treatment of the fiber surfaces by wetting agents appear not to have the intrinsic electrolyte management properties of the metal oxides.

c) Electrolyte management characteristics of the inorganic microporous mats are improved by using copolymers of ethylene-acrylic acid as a binder on Zircar cloth or (ii) mixtures of potassium titanate and zirconium oxide fibers on Zircar cloth.

ACKNOWLEDGEMENTS

Olga Gonzalez-Sanabria provided a portion of the separator characterization data in Table II.

REFERENCES

1. Abbey, K. M. and L. H. Thaller, "Pore Size Engineering Applied to Starved Electrochemical Cells and Batteries," NASA TM-82893, (1982).

2. Abbey, K. M. and D. L. Britton, "Electrotyte Management in Porous Battery Components - Static Measurements," NASA TM-83973, (1982).

3. Holleck, G. L., et al., "Ag/H_2 Energy Storage Report," AFAPL-TR-78-65, (1978).

4. "NASA Redox Storage System Development Project, 1980," DOE/NASA/12726-18, NASA TM-82940, (1982).

5. Lim, H. S., "Expansion of the Nickel Electrode," The 1980 Goddard Space Flight Center Battery Workshop, G. Halpert, ed., NASA CP-2177, pp. 175-181, NASA, Washington, D.C. (1981).

6. Unpublished data on nickel electrodes from nickel-cadmium cells cycles under Accelerated Test Program for Sealed Nickel-Cadmium Spacecraft Batteries/Cells.

7. Hunter, R. J., Zeta Potential in Colloid Science, Academic Press, London (1981).

8. Handley, L. M., et al., "Development of Advanced Fuel Cell System (Phase II)," NASA CR-134721, (1975).

9. Parks, G. A., "The Isoelectric Points of Solid Oxides, Solid Hydroxides, and Aqueous Hydroxo Complex Systems," Chem. Rev, 65(2), 177-198 (1965).

10. Verzwyvelt, S., "PBI Treated Polypropylene Battery Separatir," The 1980 Goddard Space Flight Center Battery Workshop, G. Halpert, ed., NASA CP-2177, pp. 217-223, NASA, Washington, D.C. (1981).

11. Rogers, H. H., et al., "Failure Mechanisms in Nickel-Hydrogen Cells," AFAPL-TR-77-90, (1977).

12. Smithrick, J. J., "Cyclic Life Tests and Failure Model of Nickel-Hydrogen Cells," 18th EICEC Meeting, 1983.

TABLE I. - THE POINT OF ZERO CHARGE OF SOME OXIDES[a]

Material	p.z.c. = pH_2
Quartz, SiO_2	2-3.7
Cassiterite, SnO_2	4.5
Rutile, TiO_2	6.0
Hematite (natural), Fe_2O_3	b4.8
Hematite (synthetic)	8.6
Corundum, Al_2O_3	9.0
Magnesia, MgO	12

[a](Ref. 7).
[b]Probably contaminated with SiO_2.

TABLE II. - SEPARATOR CHARACTERIZATION MEASUREMENTS

Membranes	Volume resistivity, Ωcm	Porosity, %	Electrolyte retention, %	Bubble pressure, psi	Thickness on wetting, %	OH^- diffusion, cm^2/sec^{-1}
Polypropylene	3.8	24	---	-----	18	----------
W. R. Grace (3 layers)	1.43	20.5	57	3.6	19	[a]7.1×10^{-5}
Celgard 3501 (12 layers)	21.66	49.1	152	>30	.6	[a]4.0×10^{-4}
Polysulfone (3 layers)	6.74	59.8	175	>30	0	[a]1.4×10^{-4}
Acropore NF-WA (2 layers)	8.17	48.7	137	4.0	12	[a]7.4×10^{-5}
FCGA, 5% EBL	4.08	62.1	173	19.4	33	7.8×10^{-5}
FCGA, 10% EBL	7.25	71.2	162	-----	25	----------
FCGA, 10% EAA	4.42	85.6	145	>30	25	3.7×10^{-5}
FCGA, 5% EBL on cloth	4.51	63.3	128	>30	16	1.1×10^{-5}
FCGA, 10% EAA on cloth	5.67	73.5	156	>30	18	8×10^{-4}
80% PKT, 20% ZrO_2, 10% EBL	-----	69.4	171	-----	----	1.0×10^{-4}
80% PKT, 20% ZrO_2, 10% EBL on cloth	2.66	60	116	-----	----	3.79×10^{-4}

[a]Measurement performed on only one layer of material.

TABLE III. - ELECTROLYTE DISTRIBUTION VALUES

(a) Polypropylene[a] (W. R. Grace)

	Dry weight, g	Electrolyte weight, g	Distribution, %	Saturation of individual components, %
Vacuum impregnation				
Nickel	11.2	1.80	51.1	N/A
Separator	.27	1.28	36.3	N/A
Hydrogen	2.09	.44	12.6	N/A
75.5% total cell electrolyte content				
Nickel	-----	1.91	71.8	106
Separator	-----	.56	21.3	43.7
Hydrogen	-----	.18	8.9	40.9

(b) Polyethylene[b]

Vacuum impregnation				
Nickel	11.05	2.33	44.3	N/A
Separator	1.02	2.31	44.0	N/A
Hydrogen	2.39	.61	11.7	N/A
88.9% total cell electrolyte content				
Nickel	-----	2.63	56.2	112.8
Separator	-----	1.88	40.1	81.0
Hydrogen	-----	.17	3.7	27.7
98.1% total cell electrolyte content				
Nickel	-----	2.61	50.6	112.2
Separator	-----	2.26	43.8	97.7
Hydrogen	-----	.28	5.5	46.2

(c) Celgard[b]

Vacuum impregnation				
Nickel	11.07	2.25	48.9	N/A
Separator	1.21	2.03	44.0	N/A
Hydrogen	2.39	.33	7.1	N/A
87.1% total cell electrolyte content				
Nickel	-----	2.66	65.9	117.4
Separator	-----	1.26	31.3	61.9
Hydrogen	-----	.11	2.8	34.2
94.1% total cell electrolyte content				
Nickel	-----	2.81	64.9	124.9
Separator	-----	1.33	30.8	65.6
Hydrogen	-----	.19	4.4	57.5

(d) Polysulfone[c]

Vacuum impregnation				
Nickel	12.68	1.73	38.9	N/A
Separator	.5	1.77	39.7	N/A
Hydrogen	2.57	.95	21.4	N/A
87.2% total cell electrolyte content				
Nickel	-----	1.80	46.5	104.4
Separator	-----	1.66	42.7	93.8
Hydrogen	-----	.95	10.8	43.9
96.8% total cell electrolyte content				
Nickel	-----	1.88	43.8	109
Separator	-----	1.79	41.6	101
Hydrogen	-----	.63	14.6	65.9

(e) Acropore NF-WA[b]

Vacuum impregnation				
Nickel	10.33	2.73	46.2	N/A
Separator	.784	2.33	39.4	N/A
Hydrogen	2.55	.85	14.4	N/A
89.1% total cell electrolyte content				
Nickel	-----	2.86	54.1	104.4
Separator	-----	1.95	37.0	83.7
Hydrogen	-----	.47	8.9	55.0
93.7% total cell electrolyte content				
Nickel	-----	2.88	51.9	105.3
Separator	-----	2.16	39.0	92.7
Hydrogen	-----	.506	9.1	59.3

[a]Nickel and hydrogen electrodes with a few formation cycles.
[b]Nickel and hydrogen electrodes (2600 cycles).
[c]Nickel electrode (few formation cycles) and hydrogen electrode (2600 cycles).

TABLE IV. - COMPARISON BETWEEN PREDICTED AND ACTUAL ELECTROLYTE UPTAKE

	Total electrolyte uptake 100% filling, gm	Predicted from porosities	
		Dry, gm	Wet, gm
Polypropylene	1.33	1.36	1.57
Polyethylene interseparator (3 layers)	2.31	1.97	2.43
Celgard (12 layers)	2.03	3.78	3.80
Polysulfone (3 layers)	1.76	2.62	2.62
Acropore NF-WA (2 layers)	2.33	2.91	3.87
FCGA, 5% EBL	3.13	3.94	6.30
FCGA, 10% EBL	3.06	3.94	5.25
FCGA, 10% EAA	3.15	7.04	9.33
FCGA, 5% EAA, Zircar cloth	3.11	7.11	8.72
FCGA, 5% EBL, Zircar cloth	2.74	5.95	7.14
80% PKT, 20% ZrO_2, 10% EBL	----	5.53	5.39
80% PKT, 20% ZrO_2, 10% EBL, Zircar cloth	3.80	8.99	9.27

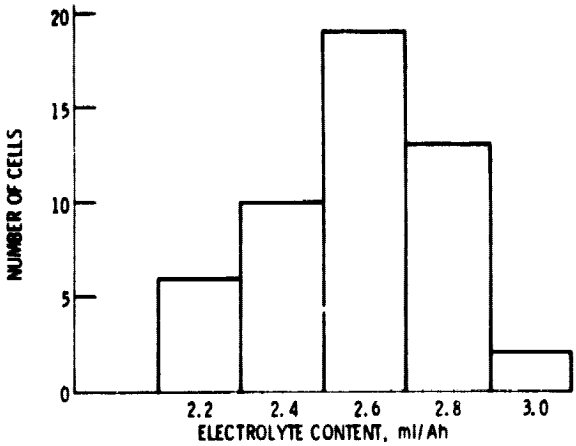

Figure 1. - Generated distribution of electrolyte volumes (Ref. 1).

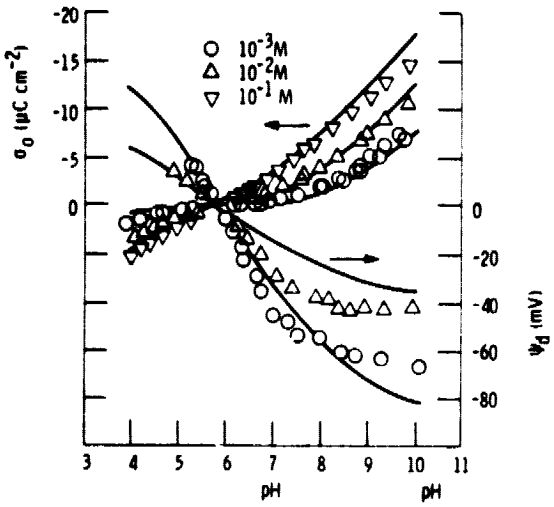

Figure 2. - The surface charge density (Yates, 1975) and ζ-potential (Wiese, 1973) of a TiO_2 dispersion as a function of pH at various concentrations of KNO_3 and at 25 C. (Ref. 7).

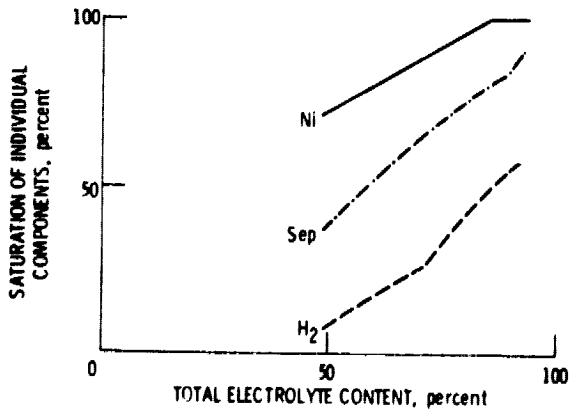

Figure 3. - Electrolyte distribution curves. Nickel electrode (2600 cycles), hydrogen electrode (2600 cycles), Acropore NF-WA separator (2 layers).

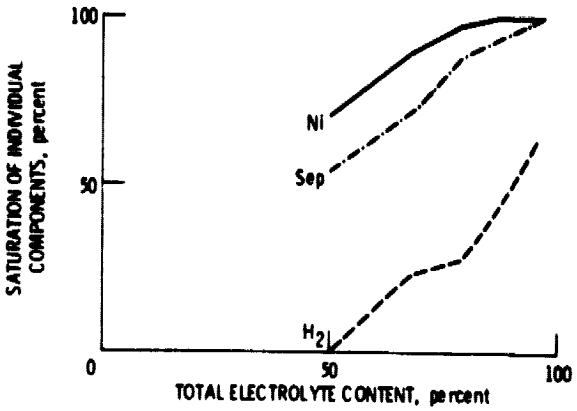

Figure 4. - Electrolyte distribution curves. Nickel electrode (few formation cycles), hydrogen electrode (2600 cycles), Polysulfone separator (3 layers).

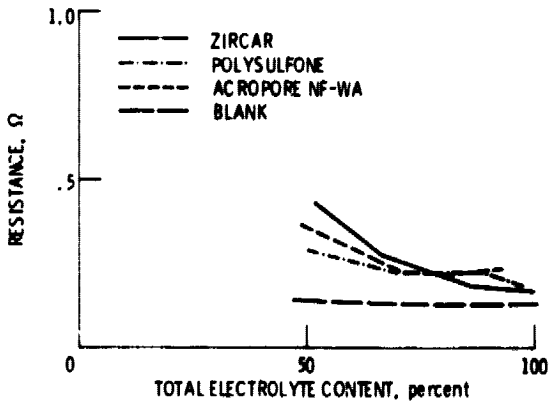

Figure 5. - Resistance as a function of cell electrolyte content. Cell consists of nickel electrode, hydrogen electrode, and separator. Blank consists of nickel and hydrogen electrodes solely.

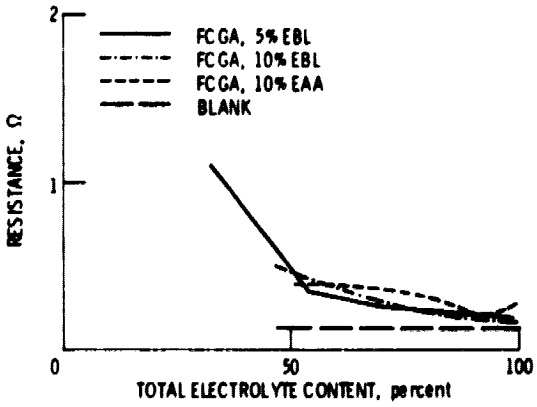

Figure 6. - Resistance as a function of cell electrolyte content. Cell consists of nickel electrode, hydrogen electrode, and separator. Blank consists of nickel and hydrogen electrodes solely.

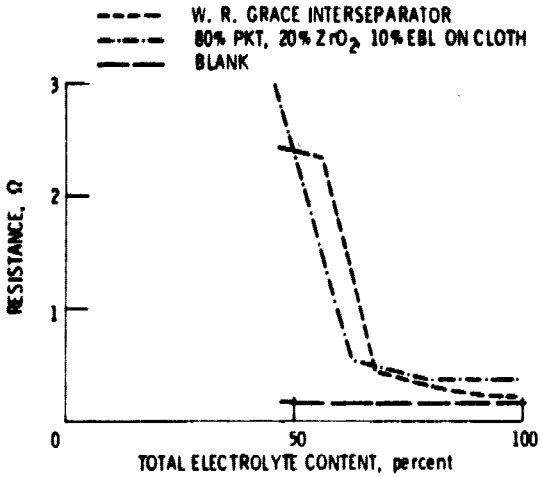

Figure 7. - Resistance as a function of cell electrolyte content. Cell consists of nickel electrode, hydrogen electrode, and separator. Blank consists of nickel and hydrogen electrodes solely.

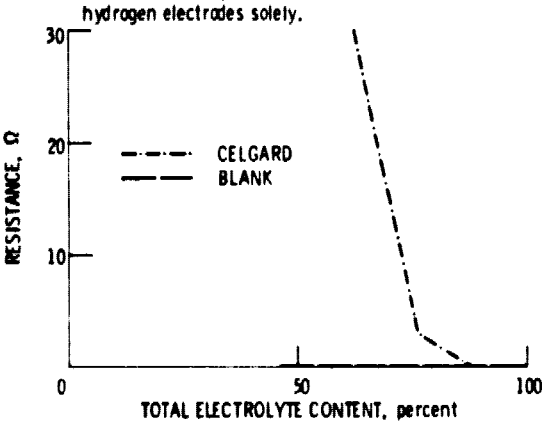

Figure 8. - Resistance as a function of cell electrolyte content. Cell consists of nickel electrode, hydrogen electrode and separator. Blank consists of nickel and hydrogen electrodes solely.

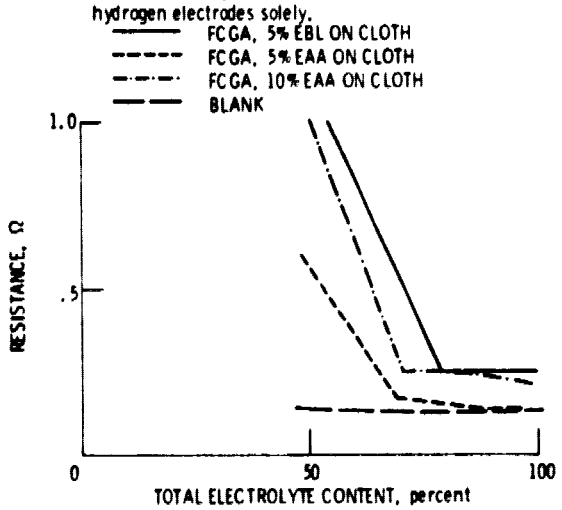

Figure 9. - Resistance as a function of cell electrolyte content. Cell consists of nickel electrode, hydrogen electrode and separator. Blank consists of nickel and hydrogen electrodes solely.

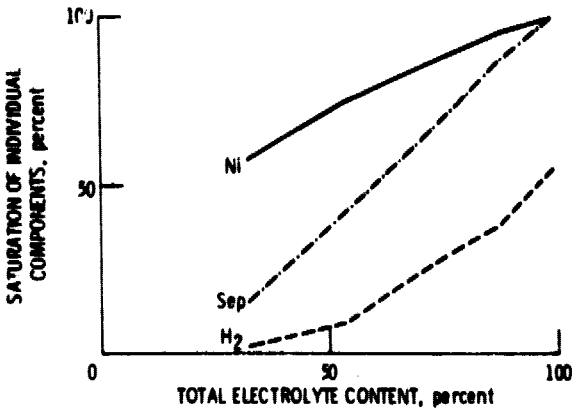

Figure 10. - Electrolyte distribution curves. Nickel electrode (2600 cycles), hydrogen electrode (2600 cycles), fuel cell grade asbestos, 5% EBL separator.

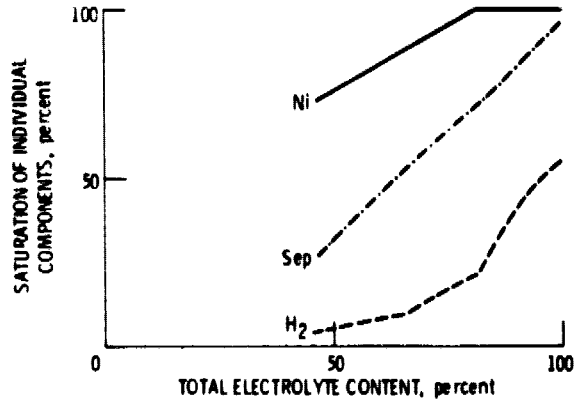

Figure 11. - Electrolyte distribution curves. Nickel electrode (2600 cycles), hydrogen electrode (2600 cycles), fuel cell grade asbestos, 10% EBL separator.

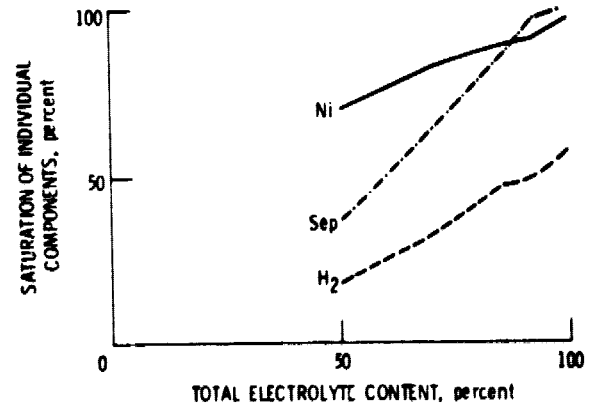

Figure 12. - Electrolyte distribution curves. Nickel electrode (2600 cycles), hydrogen electrode (2600 cycles), fuel cell grade asbestos, 10% EAA separator.

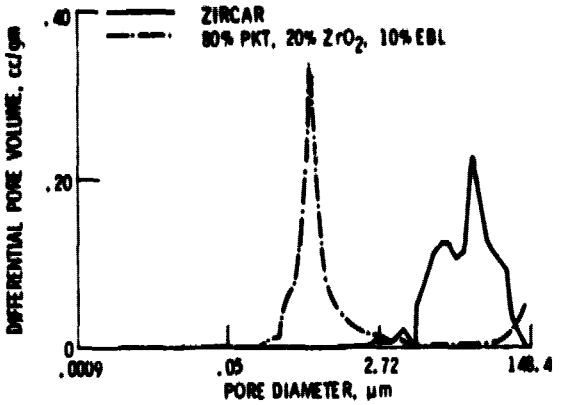

Figure 13. - Pore size distributions of separators.

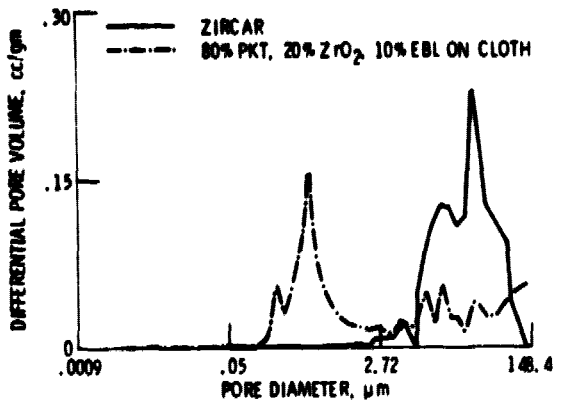

Figure 14. - Pore size distributions of separators.

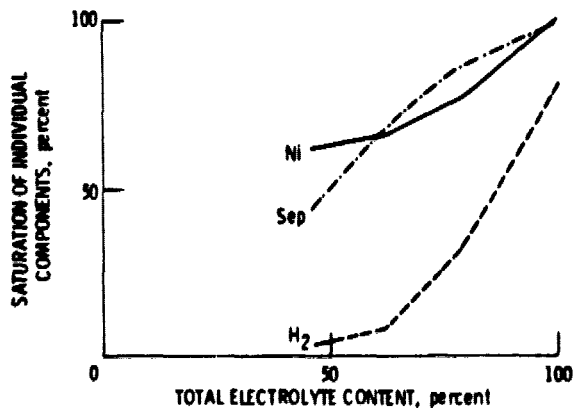

Figure 15. - Electrolyte distribution curves. Nickel electrode (few formation cycles), hydrogen electrode (2600 cycles), composite separator consisting of 80% PKT, 20% ZrO_2, 10% EBL on Zircar cloth.

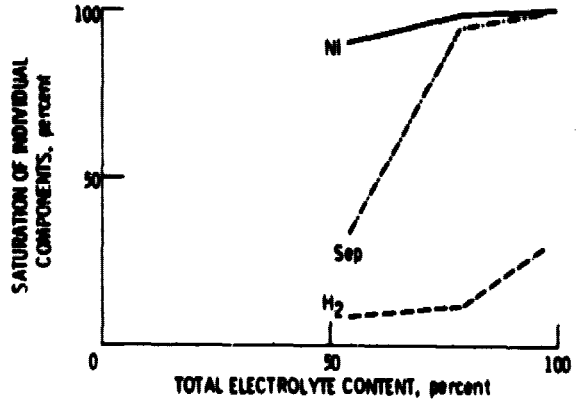

Figure 16. - Electrolyte distribution curves. Nickel electrode (2600 cycles), hydrogen electrode (2600 cycles), fuel cell grade asbestos, 5% EBL on Zircar cloth.

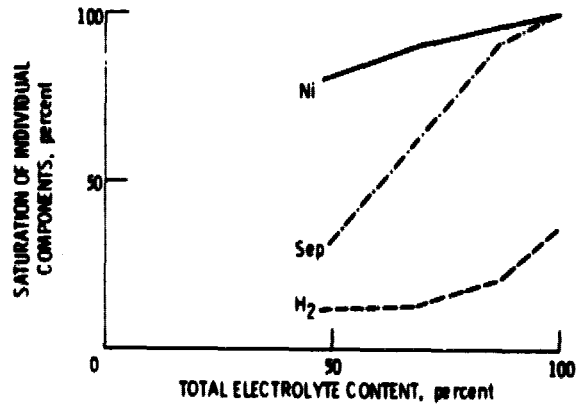

Figure 17. - Electrolyte distribution curves. Nickel electrode (2600 cycles), hydrogen electrode (2600 cycles), fuel cell grade asbestos, 5% EAA on Zircar cloth.

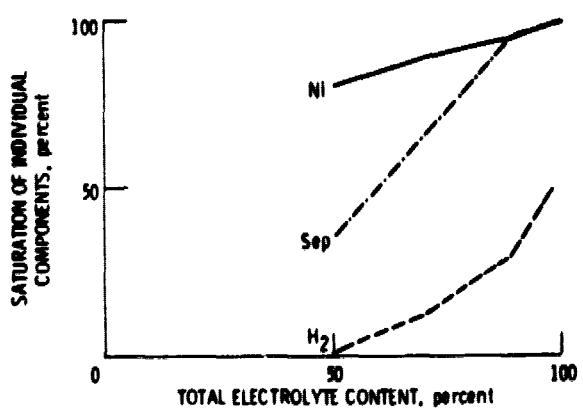

Figure 18. - Electrolyte distribution curves. Nickel electrode (2600 cycles), hydrogen electrode (2600 cycles), fuel cell grade asbestos, 10% EAA on Zircar cloth.